Evolutionary consequences of domestication on the selective effects of new amino acid changing mutations in canids

Carlos Eduardo G. Amorim[a,1,2], Chenlu Di[b,1], Meixi Lin[c], Clare Marsden[b,d], Christina A. Del Carpio[b], Jonathan C. Mah[b], Jacqueline Robinson[e], Bernard Y. Kim[f], Jazlyn A. Mooney[g], Omar E. Cornejo[h], Kirk E. Lohmueller[b,i,2]

[a]Biology Department, California State University, Northridge, California, 91330, USA

[b]Department of Ecology and Evolutionary Biology, University of California, Los Angeles, California, 90095, USA

[c]Department of Integrative Biology, University of California, Berkeley, Berkeley, California, 94720, USA

[d]Serology/DNA unit, Forensic Science Division, Los Angeles Police Department, Los Angeles CA 90032

[e]Institute for Human Genetics, University of California San Francisco, San Francisco CA 94143

[f]Department of Ecology and Evolutionary Biology, Princeton University, Princeton, NJ 08544, USA

[g]Department of Quantitative and Computational Biology, University of Southern California, Los Angeles, California, 90089, USA

[h]Ecology & Evolutionary Biology Department, University of California, Santa Cruz, California, 95060, USA

[i]Department of Human Genetics, David Geffen School of Medicine, University of California, Los Angeles, California, 90095, USA

[1]C.E.G.A and C.D. contributed equally to this work.

[2]To whom correspondence may be addressed. Email: klohmueller@ucla.edu, eduardo.amorim@csun.edu.

Competing interests statement: The authors declare no competing interests.

29

Abstract

30

31 The domestication of wild canids led to dogs no longer living in the wild but instead residing
32 alongside humans. Extreme changes in behavior and diet associated with domestication may
33 have led to the relaxation of the selective pressure on traits that may be less important in the
34 domesticated context. Thus, here we hypothesize that strongly deleterious mutations may have
35 become less deleterious in domesticated populations. We test this hypothesis by estimating the
36 distribution of fitness effects (DFE) for new amino acid changing mutations using whole-
37 genome sequence data from 24 gray wolves and 61 breed dogs. We find that the DFE is
38 strikingly similar across canids, with 26-28% of new amino acid changing mutations being
39 neutral/nearly neutral ($|s| < 1e\text{-}5$), and 41-48% under strong purifying selection ($|s| > 1e\text{-}2$).
40 Our results are robust to different model assumptions suggesting that the DFE is stable across
41 short evolutionary timescales, even in the face of putative drastic changes in the selective
42 pressure caused by artificial selection during domestication and breed formation. On par with
43 previous works describing DFE evolution, our data indicate that the DFE of amino acid
44 changing mutations depends more strongly on genome structure and organismal characteristics,
45 and less so on shifting selective pressures or environmental factors. Given the constant DFE
46 and previous data showing that genetic variants that differentiate wolf and dog populations are
47 enriched in regulatory elements, we speculate that domestication may have had a larger impact
48 on regulatory variation than on amino acid changing mutations.

Significance Statement

50 Domestication of dogs to live alongside humans resulted in a dramatic shift in the pressures of
51 natural selection. Thus, comparing dogs and wolves offers a unique opportunity to assess how
52 these shifts in selective pressures have impacted the fitness effects of individual mutations. In
53 this project, we use patterns of genetic variation in dogs and wolves to estimate the distribution
54 of fitness effects (DFE), or the proportions of amino acid changing mutations with varying
55 fitness effects throughout the genome. Overall, we find that the DFE for amino acid changing
56 mutations is similar between dogs and wolves. Even genes thought to be most affected by
57 domestication show a similar DFE, suggesting that the DFE has remained stable over
58 evolutionary time.

Introduction

60 Domestication created radical phenotypic changes in many species and understanding the
61 genetic and evolutionary basis of these changes is a major research objective (1–4). Studies on
62 animal and plant domesticates have shown that these changes are accompanied by an increase
63 in the number and frequency of deleterious genetic variants (5–7), an enrichment of identity-
64 by-descent (IBD) segments, coupled with an excess of runs of homozygosity (ROH) (8, 9), the
65 simplification of the genetic architecture of polygenic traits (7, 9), and an increase in the overall
66 recombination rates (10, 11). What remains unclear is whether domestication has also altered

2

the strength of natural selection on amino acid changing (or nonsynonymous) variants due to shifted selective pressures.

Artificial selection for desired traits during the process of domestication is thought to have led to the rapid increase in the frequency of alleles with large effects on the trait, triggering selective sweeps (7, 9, 12, 13), but may also have led to the relaxation of the selective pressure on traits that are less important in the domesticated context, such as camouflage and predator avoidance. Here, we hypothesize that strongly deleterious mutations may have become less deleterious in domesticated populations living alongside humans, while neutral mutations underlying traits of interest may have been selected by breeders, shifting the selection coefficients of genetic variants associated with these traits.

We test this hypothesis by studying the distribution of fitness effects (DFE) for nonsynonymous mutations in populations of wild wolves and breed dogs. The DFE is defined as the distribution of selection coefficients in an organism's genome (or part of its genome) and it quantifies the proportions of new mutations that are neutral, deleterious, or beneficial (14). The DFE plays a fundamental role in population genetics, with implications for the understanding of the genetic architecture of complex traits, the evolution of recombination, and the survival of threatened species of ecological concern (14–17). Moreover, it also informs about the adaptive potential of a species and the amount of background selection expected in an organism's genome (18–20). Despite its significance, our understanding of the biological factors influencing the DFE remains incomplete (21). Comparing different model organisms, Huber et al. (22) detected significant differences in the DFE across large evolutionary time scales, in particular between humans and flies. On a smaller time-scale, however, the DFE seems to be more stable. A comparative study on humans, flies, and tomatoes found that the DFE of different populations of the same species (or subspecies of the same genus) is highly correlated, with a correlation coefficient ranging from 0.91 to 0.99 (23). Importantly, their work found that the correlation is inversely related to genetic differentiation between populations. Similarly, Castellano et al. (24) found that the shape of the deleterious DFE is strikingly similar across great apes. Among the two main factors shaping the DFE are the organism complexity and the effective population size (N_e) (22, 24–26). Organism complexity – defined in terms of a larger number of unique cell types coupled with a larger genome with more genes and more protein-protein interactions – should be similar in phylogenetically related organisms. Thus, all else being equal, we would expect the DFE of closely related species, like the ones examined in refs. (23, 24) to indeed be highly correlated and similar. However, the other piece of the puzzle, namely the N_e, is known to vary across closely related species and even across populations within a species (24, 27) and thus, in principle, we can expect to see changes in DFE across short evolutionary time scales.

While our understanding of the determinants of the DFE is increasing, there are still many gaps such as how much it varies across non-model species and what factors in addition to organism complexity and N_e shape the DFE. Insights from comparing the ratio of nucleotide diversity for nonsynonymous and synonymous variants (π_N/π_S) across plant species revealed additional factors that may influence the DFE (21, 28). These features include selfing/outcrossing, longevity, reproductive system, and ploidy ((21) and references therein). While the full DFE

3

108   cannot be inferred from π_N/π_S alone, as this ratio also is affected by changes in population size,
109   these observations suggest that additional factors related to life-history traits could play a role
110   in determining the DFE of a species.

111   Domestication can impact both the life-history traits and the N_e of a species (29, 30), raising
112   the question of whether it might also alter the DFE. Additionally, although the process of
113   domestication can follow different pathways (31) and vary across and within species (1), it
114   typically entails fast and drastic changes in the selective pressure acting upon a population (1,
115   7, 32). For instance, at the early stages of domestication, selection for tameness and against
116   aggressiveness may take place as animals start living in the surroundings of human populations
117   (31, 32). Shifts in dietary intake are also expected, since animals may take advantage of the
118   resources associated with human societies such as food waste, smaller animals that are attracted
119   to it, and surplus food (31, 33). At later stages of domestication, in particular, during breed
120   formation and the improvement of traits, we expect to see fast shifts in the selective pressure
121   (1). For instance, many of the traits of interest for breeders may be deleterious in the wild –
122   such as an increase in tameness, extreme morphological alterations (e.g., brachycephaly), and
123   the loss of camouflage – which means that, in practice, humans could be selecting for traits that
124   otherwise would be eliminated in the wild. These phenomena combined, in particular the
125   changes in N_e and in the selective pressure resulting from intense artificial selection, could in
126   principle result in a shift in selection coefficients, changing the DFE in domesticates relative
127   to their wild counterpart. In this context, domesticated animals offer a unique opportunity for
128   the study of the determinants of the DFE, specifically by allowing for dissecting the relative
129   importance of drastic environmental shifts (emulated by the process of domestication and breed
130   formation) and the shared organismal characteristics of closely related species (the wild and
131   the domestic counterparts).

132   To tackle these questions, we focused on comparing the DFE of wild wolves and domestic
133   dogs. Evidence suggests that dogs were domesticated from gray wolves (*Canis lupus*) around
134   15,000 years ago or earlier (29, 34, 35), making them the oldest known domesticated species.
135   Modern dog breeds arose much more recently, around 200 years ago through multiple
136   processes involving intense artificial selection, inbreeding, and gene flow (36). Both the initial
137   domestication of dogs and the more recent development of dog breeds entailed severe
138   population bottlenecks (29, 35–37), with significant consequences to the dog genetic diversity
139   such as an excess of deleterious genetic variants (5) and runs of homozygosity (8). Here, we
140   ask whether domestication has also shifted the selection coefficients in the dog genome relative
141   to that of the wolf. We address this question by leveraging whole-genome sequence data from
142   24 gray wolves and 61 dogs. After accounting for differences in demography and background
143   selection, we find that the DFE is strikingly similar across canids, with 26-28% of new amino
144   acid-changing mutations being neutral/nearly neutral ($|s| < $ 1e-5), and 41-48% under strong
145   purifying selection ($|s| > $ 0.01). We evaluate the robustness of our results to different model
146   assumptions and conclude that the DFE is stable across short evolutionary timescales, even in
147   the face of putative drastic changes in the selective pressure caused by artificial selection during
148   domestication and breed formation. On par with previous works describing DFE evolution
149   across the tree of life, our results indicate that the DFE of nonsynonymous mutations depends

4

150 more strongly on genome structure and organismal characteristics, and less so on shifting
151 selective pressures or environmental factors.

Results

153 **Genetic Diversity in Wolves and Breed Dogs.** We analyzed four canid populations for which
154 publicly available, high-coverage (>30x), whole genome sequences were available: Arctic
155 Wolf (AW; n = 15 (38, 39)), Border Collie (BC; n = 10 (40)), Labrador Retriever (LB; n = 10
156 (40)), and Pug (PG; n = 15 (41)). Genomic VCF files were generated for each population
157 according to the pipeline outlined by Phung et al. (39)
158 (https://github.com/tanyaphung/NGS_pipeline). These VCFs were subset to exonic regions
159 considering the CanFam3.1 reference genome exon annotations. We exclusively considered
160 biallelic SNVs where all three potential variants were annotated as either synonymous or
161 missense (henceforth nonsynonymous) mutations, in practice excluding sites with potential
162 nonsense mutations, splice sites variants, and indels. This resulted in a total exonic sequence
163 length of ~21.7 Mb for which we retrieved data in the four canid populations.

164 Genetic variation data was summarized by the folded site frequency spectrum (SFS) for each
165 population, after the removal of related individuals and projecting down the sample size in
166 order to maximize the number of usable SNPs. No evidence of substantial population structure
167 within each group was detected based on a Principal Component Analysis (Fig. S1). The final
168 folded SFSs are shown in Fig. S2 and S3, highlighting nonsynonymous variants segregating at
169 lower frequency relative to synonymous mutations.

170 **Controlling for the Effects of Demography and Background Selection in the Estimation**
171 **of the DFE.** In this work, we sought to characterize the effects of changing selective pressures
172 (caused by artificial selection during the process of domestication and breed formation) on the
173 DFE of new mutations. To do so, we initially used the SFS of the wolf (AW) and three breed
174 dog populations (BC, LB, and PG) mentioned above. The SFS of a population is shaped by
175 different evolutionary forces such as genetic drift, natural selection, and background selection
176 in linked sites. To untangle the effects of target natural selection from the effects of
177 demographic changes and background selection, we followed an approach developed by Kim
178 et al. (42) consisting of two steps. First, we use the SFS of synonymous variants to infer the
179 underlying demography; and second, we use the inferred demographic model and the SFS of
180 nonsynonymous variants to infer the DFE. We implemented this approach with $\partial a \partial i$ (43), a
181 maximum-likelihood method that uses diffusion approximations to fit population genetic
182 models of demographic history and natural selection to genetic polymorphism data summarized
183 in SFS.

184 We initially considered a two-stage demographic model (henceforth, "2-epoch") allowing for
185 one instantaneous population size change, and used the multinomial likelihood to infer the
186 demographic parameters. The parameters of the model are ω – the intensity (i.e., fold-change)
187 of the population size change – and time T that this demographic change occurs in the past.
188 The method also outputs θ_S, the estimated population mutation rate for synonymous mutations,

5

189   defined as $\theta_S = 4*N_a*\mu*L$, where N_a is the estimate of the effective population size of the
190   ancestral population (before the population size change), μ is the mutation rate per site, per
191   generation, and L is the coding sequence length. The inferred demographic model parameters
192   are presented in Table S1. We infer the wolf's population N_a at ~72,000 individuals and a
193   population size reduction (ω) of approximately 19% of its size at ~2,000 generations ago.
194   Estimates for BC and LB are in the same order of magnitude, with N_a = ~52,000 and ~86,000,
195   ω = ~34% and ~20% respectively, although population size change takes place at an earlier
196   period (~17,500 generations ago in either population). The estimates for PG indicate a much
197   larger ancestral population effective size of ~223,000 and a much more severe bottleneck (ω =
198   3.5%), taking place more recently (~8,000 generations ago). Both the model and the data SFSs,
199   as well as the residuals of the model fit, are shown in Figures S4 and S5, highlighting the
200   models fit the data well.

201   **Stability of the DFE Despite Domestication.** We next inferred the DFE for new mutations
202   using the nonsynonymous SFS, conditioning on the maximum-likelihood demographic
203   parameters inferred from the synonymous variants. In doing so, we do not directly quantify the
204   selection coefficient of each variant, but instead, summarize the distribution of fitness effects
205   (DFE) over many sites. Initially, we focused on all exons annotated in the CanFam3.1 reference
206   genome assembly for this inference, in order to calculate the genome-wide DFE of
207   nonsynonymous mutations for each population of canids.

208   To infer the DFE of nonsynonymous mutations, we used *fit∂a∂i* (42), a modification of
209   *∂a∂i* (43) that allows for the inference of DFE from polymorphism data. Initially, we
210   considered that the selection coefficients (s) followed a gamma distribution and inferred its
211   shape and scale parameters. In addition to the gamma distribution, at a second stage, we also
212   considered a mixture distribution where a proportion of mutations are neutral (s = 0) and the
213   rest follow a gamma distribution ("neugamma" henceforth). We effectively treat the
214   neugamma distribution as a single integrable function, as described in ref. (42).

215   The inferred gamma-distributed DFE in canids (Fig. 1) shows no significant differences across
216   the wolves (AW; yellow) and three different breeds of dogs (BC, LB, and PG; different shades
217   of blue). The proportion of neutral/nearly-neutral mutations ($|s|$ < 1e-5) is ~26-28% across
218   wolves and dogs and that of strongly deleterious mutations ($|s|$ > 1e-2) is ~41-48% (Table S2).
219   No statistically significant differences between the discretized DFE were observed across canid
220   populations, based on the overlap of the 95% confidence intervals (Fig. 1).

221   Assuming a neugamma distribution for the DFEs, we observe a similar pattern, although the
222   confidence intervals are considerably larger (Fig. S6). While the neugamma distribution
223   improves the fit of the model for some populations (Table S3), we found that the optimizations
224   for the neugamma did not converge as well as the ones for the former. On a related note, when
225   we compare the DFEs of these four canid populations considering the distribution with best
226   log-likelihood in each case (namely gamma for BC and neugamma for the other three
227   populations), we still see no significant differences in the DFEs across populations when
228   considering the 95% confidence interval (Fig. S7), although the neugamma DFE for PG

6

229   predicts a considerably higher proportion of strongly deleterious mutations than that in the
230   other populations. The estimated parameters of the gamma and neugamma DFEs for the
231   analyses, as well as the corresponding log-likelihoods, are reported in Tables S2 and S3. The
232   model SFS fits for the nonsynonymous SFS for both the gamma and neugamma distributions
233   and corresponding residuals are shown in Figures S8-S11, indicating the inferred DFE models
234   fit the data well considering either functional form of the DFE.

235   We observed a similar pattern when we use the same sample sizes of $n_{eq} = 6$ across all four
236   populations (Fig. S12), although the 95% confidence intervals are wider, as expected due to
237   the reduced data. Finally, we computed the population-scaled DFE, $2N_a s$, for the four canid
238   populations. Estimates of $2N_a s$ measure the relative strengths of selection vs. drift acting in the
239   population and are more robust than estimates of s, as $2N_a s$ is directly inferred from $fit\partial a\partial i$.
240   Similar to the population-scaled DFE in terms of s, we detect no significant differences in the
241   DFE across AW, BC, LB, and PG (Fig. S13). In sum, the inference of a stable DFE for
242   nonsynonymous mutations in canids is not an artifact caused by different sample sizes across
243   populations or biases in converting estimates of $2N_a s$ into estimates of s.

244   **The Wolf and Dog DFEs are Highly Correlated.** Because dogs and wolves have diverged
245   relatively recently (29, 34, 35), and we did not observe any differences in the DFE between
246   dogs and wolves, we sought to jointly model their DFE, following the approach developed by
247   Huang et al. (23). According to this approach, the joint DFE is estimated for pairs of
248   populations, and the correlation of their selection coefficients (ρ) is estimated. That is to say, ρ
249   = 1 means that the mutations have the same selection coefficients in both populations, while
250   lower values of ρ indicate that those mutations that are deleterious in one population may not
251   be deleterious in the second population. This approach follows the same framework of
252   $\partial a\partial i/fit\partial a\partial i$, using the synonymous SFSs to control for the effects of demography and
253   background selection, and the nonsynonymous SFSs for the DFE inference, except that it uses
254   the joint SFS (i.e., 2-dimensional; henceforth "2D"), computed for a pair of populations (23).
255   The method requires only modest sample sizes and is robust to many forms of model
256   misspecification (23).

257   We first fit a simple demographic model ("split_mig") with a population split at time T in the
258   past (Fig. S14-S16). According to this model, the size of the two derived populations relative
259   to the ancestor is ω_1 and ω_2, and remain constant after the split. Symmetric migration between
260   the two derived populations happens at a rate m. We consider the following pairs of
261   populations: AW-BC, AW-LB, and AW-PG. Projected sample sizes are the same used for the
262   single population analysis described above. The joint SFS and fit plots are found in Figures
263   S14-S16 and the inferred demographic parameters, in Table S4. The 2D demographic models
264   show similar joint inferred demography across each pair, with $N_a = $ ~20,500, effective
265   population size in the present (N_p) for the wolf population after the split at ~8,400, and split
266   time at ~4,000 generations ago. The only noticeable difference across the three models is the
267   N_p for the breed dog populations after the split, which ranges from ~500 for PG to
268   approximately 1,300 for BC and LB (Table S4).

7

269 We inferred the joint DFE using the joint SFS of nonsynonymous variants (Fig. S17-19). Since
270 little is known about the joint DFEs of wolf and breed dog populations, we first considered a
271 simple bivariate lognormal distribution with an easily interpretable correlation coefficient.
272 Given the similarity in DFEs for single populations, we assumed a symmetric bivariate
273 lognormal distribution in which the marginal DFE for the wolf and dog populations are the
274 same, while the parameter ρ quantifies the correlation of fitness effects of mutations between
275 populations. Using a Poisson likelihood framework, we inferred the DFE parameters for each
276 wolf-dog population pair (Table S4). We found that the DFEs of wolf and dog across all three
277 comparisons are perfectly correlated ($\rho > 0.99$; Table 1). The discretized DFE for the bivariate
278 lognormal joint DFEs and single-population gamma DFEs predict similar proportions of
279 mutations in each bin (Table 1), suggesting the robustness of our findings relative to the
280 assumptions about the functional forms of the DFE and whether we model the populations
281 separately or jointly.

282 **Assessing the Robustness of the Inferred DFE.** In order to confirm our observations about
283 the stability of the DFE despite domestication, we sought to replicate our results using a
284 separate dataset comprising one wolf and two dog populations. The wolf population (MW)
285 comprises the genomes of nine gray wolves sequenced at ~19x depth of coverage (5). The two
286 dog populations comprise one sample with 20 domestic breed dogs (MD) sequenced at an
287 average of ~18x (5) and 10 Tibetan mastiffs (TM) sequenced at ~15x (39). Only one individual
288 was removed from TM due to relatedness with other TMs in the sample. Following the same
289 approach used for the higher coverage data (namely AW, BC, LB, and PG), we projected down
290 the sample size in order to maximize the number of usable sites. The final sample sizes after
291 projection and removal of related individuals are MW = 8, MD = 16, and TM = 7.

292 We fit a 2-epoch demographic model to the synonymous SFS (Table S1; Fig. S4 and S5) and
293 a gamma-distributed DFE model to the nonsynonymous SFS (Table S2; Fig. S8 and S9) using
294 $\partial a \partial i/fit\partial a \partial i$. Although the maximum likelihood estimates for the proportion of new
295 mutations with different values of s may appear to differ between wolves (MW) and dogs (MD
296 and TM) using this lower coverage dataset (Fig. S20), the 95% confidence intervals of these
297 estimates overlap, suggesting no significant differences between the DFEs of MW, MD, and
298 TM. This observation confirms our findings obtained with the analysis of the high coverage
299 samples (Fig. 1) showing no significant differences in the DFE of wolves and dogs.

300 In addition to confirming the observations of a stable DFE in canids with an independent
301 dataset, we also assessed whether misspecification in the model parameters could bias our
302 estimates. We did so by using the high coverage samples (AW, BC, LB, and PG), considering
303 their full, projected sample sizes, and re-ran the analyses considering a low mutation rate of
304 3.00e-9 (considering the lower range of the estimate from ref. (35)), a high mutation rate of
305 6.73e-9 (considering the cat-dog divergence-based mutation rate from ref. (39)) and a 1.25x
306 higher mutation rate in exons – see Materials and Methods), the expected ratio of
307 nonsynonymous-to-synonymous mutations (NS:S) estimated for humans (42), and a 3-epoch
308 demographic scenario (Table S5).

309   The inferred DFE for dogs and wolves in each case are highly similar (Fig. S21), confirming
310   our observations are robust to misspecification of the model, as far as it concerns the mutation
311   rate (within a reasonable range for canids (35, 39)), the expected NS:S ratio (within a
312   reasonable range for mammals (42)), and the number of population size changes. We note that
313   the log-likelihood of the inferred 3-epoch demographic model for PG is slightly improved
314   relative to that of the 2-epoch model (log-likelihood = -79.59 and -72.95 respectively);
315   however, the gamma DFE for PG is qualitatively similar regardless of the demographic model
316   considered (Fig. S22).

317   **DFE Inference for Domestication-associated Genes.** While our results using the whole dog
318   exome point to no differences in the DFE of nonsynonymous mutations in dogs and wolves
319   (Fig. 1), even when considering different model assumptions and population samples (Table 1,
320   Fig. S6, S12, S20, and S21), we hypothesized that the effects of domestication on the DFE may
321   be more pronounced in gene sets thought to be associated with domestication. Although no
322   single suite of traits is consistently seen across domestic animals (44), the literature harbors a
323   number of studies evidencing signals of natural selection in domesticated species associated,
324   in particular, with the nervous system, behavioral traits, skeletal system development,
325   immunity, and pigmentation (7, 12, 13, 29, 32, 45, 46). Thus, to tackle this question, we subset
326   the whole-exome data to different sets of genes implicated in pathways putatively associated
327   with domestication.

328   To implement this approach, the whole-exome data were filtered based on the following Gene
329   Ontology terms: Nervous System Development (5.5 Mb exonic sequence length), Immune
330   System Processes (3.6 Mb), and a combination of Immune System Processes, Nervous System
331   Development, Carbohydrate Metabolic Processes, Pigmentation, and Skeletal System
332   Development ("Domestication Genes" subset; 10.4 Mb). Similarly to our previous analyses,
333   we fit first the synonymous SFS from the genes in each set in AW, BC, LB, and PG
334   (considering the maximum sample size projected) to 2- and 3-epoch demographic models.
335   Based on log-likelihoods estimated by $\partial a \partial i$, we picked the best demographic model for each
336   population considering each gene set independently for a total of 12 models (Tables S1 and
337   S5). We assume a gamma-distributed DFE and fit the resulting model SFS to the data
338   nonsynonymous SFS following the same procedure adopted for the whole exome analysis.

339   The discretized gamma-DFE computed for each gene set shows no significant differences in
340   the predicted proportion of deleterious and neutral mutations at different selection strengths
341   (Fig. 2). While small differences in the maximum-likelihood estimates for these proportions
342   are visually evident in some cases, in particular showing a larger proportion (additional ~10%)
343   of strongly deleterious mutations in PG relative to the others for the Nervous System
344   Development and "Domestication Genes" sets, the 95% confidence intervals largely overlap
345   (Table S6).

Discussion

The Evolutionarily Stable DFE of Dogs and Wolves. Our findings allow us to revisit our initial hypothesis that shifts in selective pressures during domestication would change the DFE in domesticated species compared to their wild relatives. We specifically hypothesized that strongly deleterious mutations might have become less deleterious under domestication and that this would have an impact in the DFE of new amino acid changing (nonsynonymous) mutations. At the early stages of domestication, selection for tameness may take place as animals start living in the surroundings of human populations (31, 32). At later stages, we expect to see fast shifts in the selective pressure (1), with many of the traits selected by breeders being potentially deleterious in the wild. Comparing populations of wolves and domestic dogs, we sought to test whether these putative shifts in selective pressure would also have an impact on the DFE of dogs. Contrary to our initial expectations, our data showed striking stability of the DFE across wild and domestic canid populations (Fig. 1), suggesting that domestication and the development of breeds may not drastically alter selection coefficients in nonsynonymous mutations, as inferred from polymorphism data. We assessed the robustness of our findings relative to differences in sample sizes across populations (Fig. S12) and model assumptions (Fig. S6 and S21; Table 1), and replicated our findings with an independent dataset (Fig. S20), and consistently observe statistically similar DFEs across wolves and breed dogs.

This stability in the DFE across wolves and dogs aligns with previous studies comparing DFE evolution across the tree of life, which have found that significant differences in the DFE occur primarily across distantly related species (22, 47), whereas minimal changes are observed among more closely related species, subspecies, or populations (23, 24, 48, 49). Insights from comparing the ratio of nucleotide diversity for nonsynonymous and synonymous variants (π_N/π_S) across plant species also pointed to a limited role of domestication on shifting selection coefficients in plants (21, 28). The observed stability of the DFE within short evolutionary time scales supports the idea that the DFE is influenced more strongly by intrinsic organismal characteristics (e.g., organismal complexity, genome structure, genetic context, life history, etc.) than by extrinsic environmental factors (21, 22, 28), here, emulated by domestication.

Despite evidence showing stability of the DFE, in particular in closely related species and populations (23, 24, 48, 49), experimental evolution studies in *Drosophila* (50) and the bacterium *E. coli* (51) indicate that environmental shifts can influence the DFE. In particular, Wang et al. (50) showed that especially the variance, V(s), of the DFE of *Drosophila* was dependent on the environment. On a similar note, the strength of natural selection on pigmentation genes was found to be different across human populations (52). Thus, while the effects of domestication and breed formation on the DFE of canids appear minimal in our study, environmental factors may still play a role under certain evolutionary contexts. Motivated by these observations, we sought to investigate the effects of domestication on gene sets in biological pathways thought to be impacted by domestication in animals, in particular, the nervous system, skeletal system development, immunity, metabolism/diet, and pigmentation (7, 12, 13, 29, 32, 45, 46). Surprisingly, we found that the DFE is stable even when analyzed for these gene sets (Fig. 2), suggesting artificial selection may not have affect the DFE of canids, even for domestication-associated gene sets.

10

One potential explanation for the observed DFE stability is that domestication-related shifts in selective pressure have not been sufficient to generate detectable changes in the DFE, at least within the sample sizes and timescales studied. Forward simulations by Castellano et al. (53), modeling pig domestication over 10,000 generations, suggest that the DFE of deleterious mutations can be accurately estimated using either the 1D and 2D SFSs–that is either modeling one population at a time or two populations jointly. In their simulations, the evolutionary effects produced by domestication are modeled by changing, at the time of the split, the fitness effects of a proportion (5% or 25%) of the existing and new mutations in the domestic population relative to the wild counterpart. Given their findings, our research design appears to be well-powered for detecting meaningful DFE changes in canids, assuming similar dynamics to what they simulated also apply to dog domestication.

Alternatively, domestication might have more pronounced effects on other mutation types, such as regulatory variants or complex structural variants, rather than the nonsynonymous mutations studied here. Indeed, variants that differentiate wolf and domestic dog populations are enriched in regulatory elements such as promoters and enhancers (54), suggesting that a promising area for further investigation is to look at DFE differences between dogs and wolves focusing on regulatory variation. Finally, it is possible that domestication and artificial selection during dog breed formation have had a greater impact on beneficial mutations (55) or standing deleterious variation, which we did not specifically assess in this study. Further analyses targeting beneficial DFE components, as well as standing variation, may provide additional insights into the evolutionary consequences of domestication in canids.

We note that the sample sizes used for our inference, ranging from $n = 6$ (n_{eq}) to 16 (MD after projection), may also limit power to detect subtle shifts in natural selection, as strongly deleterious variants are expected to segregate in low frequencies and thus not be observed in our sample. Instead, the strongly deleterious part of the DFE is extrapolated from the lack of common variants and the functional form of the DFE assumed. Larger sample sizes including more rare variants could enable more accurate inference of the more strongly deleterious part of the DFE. However, we note that estimates of the proportion of neutral/nearly neutral variants ($|s| < $ 1e-5) among new mutations is less likely to be impacted by sample size. For this portion of the DFE, where we have more information, we do not detect a difference across wolves and breed dogs. This finding suggests that if we assume the DFE of new mutations is gamma distributed, we can use data from a small number of individuals to learn about mutations that we did not observe in our sample.

The canid DFE relative to other animals. A recent study analyzed the DFE across eleven animal (sub)species, including humans, mice, fin whales, vaquitas, gray and Arctic wolves, collared flycatchers, pied flycatchers, halictid bees, *Drosophila*, and mosquitoes (56). Their findings show variation in the DFE across deep evolutionary time, with mammals having a larger proportion of strongly deleterious ($|s| > $ 1e-2) mutations (22% in vaquitas to 47% in Arctic wolves) than other animals (0.0% in *Drosophila* to 5.4% in collared flycatchers), while the proportion of weakly deleterious mutations (1e-5 $\leq |s| < $ 1e-3) is smaller in mammals relative to birds and insects (56). Previously, Huber et al. (22) examined five competing models

11

429 explaining the determining factors driving DFE evolution and found strong support for the
430 Fisher's Geometrical Model (FGM). According to the FGM, phenotypes are characterized as
431 points in an n-dimensional space, with fitness being a decreasing function of the distance from
432 the optimal phenotype (57). The phenotype dimensionality n can be understood as the
433 "organismal complexity." Among others, the FGM makes one key prediction that is confirmed
434 by refs. (22, 56) that mutations in more complex organisms are on average more deleterious
435 because they are more likely to disrupt an important function in a complex organism than in a
436 simpler one. In this context, the unusually high proportion of strongly deleterious mutations
437 ($|s| > $ 1e-2) in canids inferred in this study (41-48%) relative to other mammals (30% fin whale,
438 27% human, 24% mouse, and 22% vaquita (56)) suggest a venue worthy of further
439 investigation.

440 **DFE and Homologous Recombination in Canids.** We speculate that our findings on the large
441 amount of predicted strongly deleterious mutations in dogs and wolves relative to other
442 mammals, including humans, may relate to the unique recombination landscape in canids,
443 where recombination predominantly occurs in promoter regions due to a non-functional
444 *PRDM9* gene (58). This recombination pattern differs significantly from other mammals,
445 where the PRDM9 protein localizes recombination hotspots throughout the genome (59, 60).
446 In species harboring a functional copy of *PRDM9*, recombination hotspots may localize
447 anywhere in the genome. The restriction of recombination to promoter regions in canids may
448 thus effectively reduce recombination within genes, potentially impacting the purging of
449 deleterious mutations under Muller's Ratchet hypothesis, which posits that low-recombination
450 regions are more prone to accumulating harmful mutations (61, 62). We note that less
451 efficiently purging deleterious mutations does not necessarily equate to a more deleterious
452 DFE. However, because our inference is based on polymorphism data, linkage between
453 mutations within genes could skew the SFS, resulting in a larger proportion of deleterious
454 mutations being inferred.

455 As a first step into examining the relationship between the DFE and recombination rates, we
456 inferred an LD-based recombination map for the Arctic wolf and subset its genome into three
457 different datasets based on the estimated recombination rates (r), in units of recombination
458 events per bp per generation: Low ($0 \leq r < $ 1.9e-9), Moderate (1.9e-9 $\leq r < $ 4.3e-9), and High
459 ($r \geq $ 4.3e-9) recombination rate. We then used these three subsets to infer the DFE using the
460 same framework implemented for the whole exome. Our results show qualitatively similar
461 DFEs between low and high recombination regions, with regions with moderate recombination
462 rate presenting an overall larger proportion of deleterious mutations (Fig. S23). One potential
463 explanation for this observation is that intermediate recombination rate regions could have
464 genes with different functions than other portions of the genome. We note that, due to the small
465 sample sizes considered in our study, our findings regarding the differences in the proportion
466 of strongly deleterious mutations across regions with different recombination rates should be
467 considered with care. On the other hand, estimating the proportions of nearly neutral variants
468 among new mutations is less likely to be impacted by sample size, and in the case of nearly
469 neutral sites ($|s| < $ 1e-4), we inferred highly similar proportions for the whole exome (33%) and
470 the different recombination subsets (Low r = 34%; Moderate r = 29%; High r = 32%). Given

12

471   the importance of recombination in shaping genetic variation, understanding how the unique
472   canid recombination pattern within mammals affects the DFE could provide valuable insights
473   into the determinants of the DFE and the implications of PRDM9-independent recombination
474   on adaptive potential and the purging of detrimental variants.

Conclusion

476   Overall, our study provides evidence that the DFE of nonsynonymous mutations remains
477   relatively stable despite the significant shifts in selective pressures putatively associated with
478   domestication in canids. Our finding underscores the role of intrinsic organismal characteristics
479   in shaping the DFE, while environmental factors and shifts in the selective pressures associated
480   with domestication may have limited influence – contradicting previous findings in *Drosophila*
481   and *E. coli* showing an influence of the environment in shaping the selecting effects of
482   nonsynonymous mutations (50, 51). Future studies could explore the full properties of the DFE
483   in other domesticated species with varying degrees of selection intensity and different life
484   history traits to determine whether these observations hold across domesticated lineages.
485   Additionally, investigating the DFE of gene promoters and enhancers in domesticated species
486   could yield further insights into the importance of natural selection on regulatory variation
487   during domestication. In conclusion, while domestication has clearly impacted genetic
488   diversity and allele frequencies in canids (and other domesticated species alike), our data
489   suggest that the DFE of nonsynonymous mutations remains resilient to these shifts, providing
490   new perspectives on the stability of fitness effects even in the face of drastic environmental
491   shifts.

Materials and Methods

493   **Genomic Data.** Whole-genome sequencing data were aggregated from the literature: Arctic
494   wolf (AW; n = 15) with ~39x coverage (38, 39), border collie (BC; n = 10) with ~24x coverage
495   (40), labrador retriever (LB; n = 10) with ~30x coverage (40), pug (PG; n = 15) with ~47x
496   coverage (41), and Tibetan Mastiff (TM; n = 10) with ~15x coverage (39). In addition to these,
497   we also aggregated data from nine wolves from different populations (referred to as "mixed
498   wolves" or MW in this study) with ~19x coverage and 20 dogs from 20 different breeds
499   (referred to as "mixed dogs" or MD in this study) with ~18x coverage (5). The term "mixed"
500   here refers to the fact that these individuals came from different populations and were pooled
501   into one sample, not that they are necessarily wolf-domestic dog hybrids or mixed breed dogs.

502   Raw whole genome sequences (*fastq* files) were processed following GATK best practices,
503   and according to the pipeline outlined by Phung et al. (39)
504   (https://github.com/tanyaphung/NGS_pipeline). In brief, the *fastq* files were first aligned to the
505   dog genome (CanFam3.1) with *BWA* (63). We then marked duplicate reads with Picard tools
506   (https://broadinstitute.github.io/picard/), removed reads with mapping quality (MAPQ) less
507   than 30 using *SAMtools* (64), and recalibrated the base quality scores using the *BQSR* tool in
508   *GaTK* v3.8 (65, 66). We performed joint genotyping with the *HaplotypeCaller* method and
509   emitted all sites (variant and invariant). To reduce bias in SNP calling accuracy between canids

from a given dataset, we conducted joint genotyping considering all individuals in each population. For example, joint genotyping was conducted on the 15 AW samples as a group, separately on the 10 BC samples as a group, and so on. We then applied post hoc filtering to each of the VCF files generated for each of the seven datasets. Specifically, we applied GATK filtering recommendations for variant sites in non-model species: QD < 2.0, FS > 60.0, MQ < 40.0, MQRankSum < -12.5, ReadPosRankSum < -8.0, and a minimum genotype quality (GQ) of 20. Additionally, we removed clustered SNPs (i.e., > 3 SNPs within 10 bp).

For invariant sites, for which no best practices were available, we applied the following filters: QUAL < 30, and RGQ < 1. For both variant and invariant sites, we applied a minimum depth filter of 10 for each genotype, as previous work has found heterozygous calls are unreliable below this depth (5), and a maximum depth filter of 2.5 times the average genomic coverage (specific for each of the seven datasets). Finally, we removed any sites where all individuals were heterozygous, fewer than 80% of individuals in a group had a genotype call after post hoc filtering was applied, or any sites within the UCSC repeat regions.

Genomic VCF files were subset to autosomal exonic regions with *VCFtools* (67). Exon coordinates for the reference dog genome *canFam3* were obtained from http://hgdownload.soe.ucsc.edu/goldenPath/canFam3/database/ensGene.txt.gz (accessed on 02/05/2018). From this dataset, we obtained the coordinates for the exons of 30,784 genes, considering the longest transcript in each case. Based on the *canFam3* reference genome, we calculated the total exon length for dogs as 25.16 Mb.

To annotate the effects of all potential exonic single nucleotide variants (SNVs), we artificially introduced "mutations" to a VCF file containing dog exome data, so that all three potential SNVs were observed in each site. The functional effects of each variant in each site were predicted with *SnpEff* (68, 69), using the dog reference genome build CanFam3.1.75, available with *SnpEff*. We used these annotations to classify each exonic position into either a 0-, 2-, 3-, or 4-fold degenerate site. We exclusively considered exonic sites where all three potential SNVs were annotated as either synonymous or nonsynonymous (missense) mutations (~21.7 Mb), effectively discarding sites with other types of annotations, such as splice sites and nonsense mutations (i.e., stop-gained and stop-lost).

Computing the Site Frequency Spectra. We used *KING* (70), implemented in *PLINK* (71), to identify pairs of related individuals and excluded those with more than 35% of their genome with at least one allele in IBD in practice removing first-degree relatives (i.e., parent-child and siblings). Relatedness was estimated using a set of putative neutral SNVs from ref. (39). To select putative neutral regions in the dog genome, these authors filtered out any locus 0.4 cM away from conserved regions, annotated with *phastConsElements100way* UCSC Genome Browser, or a gene, resulting in approximately 24.5 Mb of sequence. The following individuals were excluded from the downstream analysis after removing related individuals: AW14, BC2, BC8, BC10, and TM4. The final sample sizes obtained for each population after the removal of one of the relatives were AW = 14, BC = 7, LB = 10, PG = 15, MW = 9, MD = 20, and TM = 9.

14

550   Because we allowed some missing data in our dataset and considering we cannot use missing
551   data to calculate the SFS, we projected down these sample sizes in order to maximize the
552   number of SNVs available for each population. We used *EasySFS*
553   (https://github.com/isaacovercast/easySFS; (43)) to calculate the number of SNVs for a given
554   sample size and to project down the sample size. *EasySFS* averages allele absolute frequencies
555   over all possible combinations of samples for a given sample size (i.e., the hypergeometric
556   projection method). The resulting projected sample sizes were: AW = 13, BC = 6, LB = 9, PG
557   = 14, MW = 8, MD = 16, and TM = 7. Additionally, to assess if unequal sample sizes were
558   biasing results, we further projected down these sample sizes to n_{eq} = 6 for the high coverage
559   samples (AW, BC, LB, and PG).

560   Based on these sample sizes after filtering and projection, we calculated the folded SFS for
561   each population using *EasySFS*. The folded SFS describes the number or proportion of variants
562   at different minor allele frequencies in the sample. We chose to use the folded SFS (as opposed
563   to the unfolded) to avoid biases resulting from the misspecification of the ancestral allele (72).

564   **Calculating Synonymous and Nonsynonymous Sequence Lengths.** After classifying each
565   exonic position into 0-, 2-, 3-, or 4-fold degenerate sites, we calculated the ratio of
566   nonsynonymous sequence length to synonymous sequence length ($L_{NS:S}$) in the *canFam3*
567   genome assembly. We used $L_{NS:S}$ to calculate the expected number of nonsynonymous
568   mutations from the inferred synonymous mutation rate for the DFE inference (see below).

569   The nonsynonymous sequence length (L_{NS}) was calculated as the number of 0-fold degenerate
570   sites, ⅔ of the 2-fold degenerate sites, and ⅓ of the 3-fold degenerate sites. Conversely, the
571   synonymous sequence length (L_S) was calculated as the number of 4-fold degenerate sites, ⅔
572   of the 3-fold degenerate sites, and ⅓ of the 2-fold degenerate sites. Because methylated CpG
573   sites are highly mutable (73, 74) and enriched in exons (as seen in humans (75)), we calculated
574    $L_{NS:S}$ considering a 10x higher mutation rate in putatively methylated CpG sites. We defined
575   putatively methylated CpG sites as those CpG sites not in CpG islands, which are known to be
576   unmethylated (76, 77). CpG islands coordinates in the dog genome were obtained from
577   http://hgdownload.soe.ucsc.edu/goldenPath/canFam3/database/cpgIslandExt.txt.gz (accessed
578   03/20/2018). This information was used for exploring the effects of different $L_{NS:S}$ in the
579   estimates of the DFE in different populations, using $L_{NS:S}$ = 2.21 calculated for the dog (this
580   study) and $L_{NS:S}$ = 2.31 calculated for the human genome (22).

581   **Demographic and DFE Inference.** We inferred demography and the DFE from site frequency
582   spectrum (SFS) according to a maximum likelihood approach in two steps. First, we inferred
583   the parameters of a demographic model considering synonymous variants. Second, we inferred
584   the parameters of the DFE of nonsynonymous variants conditional on the demographic
585   inference. As shown by Kim et al. (42), this two-step approach effectively controls for the
586   effects of demography and background selection when estimating the DFE of nonsynonymous
587   variants. The rationale behind this approach is that, if nonsynonymous variants are completely
588   neutral, the SFS computed based on these variants will have the same shape as the SFS of
589   synonymous variants and the number of nonsynonymous mutations will be 2.21x larger (for
590   dogs, as calculated in the present study). Any differences between the shapes of the

15

591 synonymous and nonsynonymous SFSs or a deviation in the number of mutations from the
592 expected can be attributed to the effects of natural selection. That is because both synonymous
593 and nonsynonymous variants are subject to the same demography. Note that, although the
594 demographic model inferred in the first step may be biased by linked selection (78), using this
595 combination of synonymous and nonsynonymous variants allows us to control for the effects
596 of background selection in addition to demography when inferring the DFE in the last step (22,
597 42).

598 We implemented both the demographic and DFE inferences using *varDFE*
599 (https://github.com/meixilin/varDFE; (56)), a robust but flexible workflow implemented in
600 Python. The demographic inference was performed with $\partial a \partial i$ (43), implemented via *varDFE*
601 (*Demog1D_sizechangeFIM* module). The method implemented via $\partial a \partial i$ uses a diffusion
602 approximation to compute the SFS given a demographic model. The multinomial likelihood is
603 maximized to estimate the demographic parameters from the observed (data) synonymous SFS.
604 A population mutation rate for synonymous variants θ_S is estimated by scaling the optimized
605 SFS relative to the observed synonymous SFS. The ancestral population size N_a can then be
606 estimated considering θ_S according to this equation: $\theta_S = 4*N_a*\mu*L$. *varDFE* uses N_a for scaling
607 the time and size parameters of the demographic model as well as the selection coefficients
608 inferred at the final step.

609 We considered two simple demographic models with spontaneous size changes. The 2-epoch
610 model has a single size change and the 3-epoch model has two size changes. As can be seen in
611 Figures S4 and S5, the SFSs computed from these simple demographic models present a good
612 fit to the observed synonymous SFSs.

613 We used $fit\partial a\partial i$ (42), implemented via *varDFE* (*DFE1D_refspectra* and
614 *DFE1D_inferenceFIM* modules), to estimate the DFE from the nonsynonymous SFSs,
615 conditioning on the maximum-likelihood estimates of the demographic parameters. The
616 method implemented with $fit\partial a\partial i$ fits a DFE to the nonsynonymous data SFS by maximizing
617 the Poisson likelihood (42). Because the Poisson likelihood requires a mutation rate for
618 nonsynonymous variants (θ_{NS}), we multiplied the estimates obtained for θ_S by the ratio of
619 nonsynonymous-to-synonymous mutation we estimated for the dog genome (2.21:1) and later
620 also for the one calculated for the human genome (2.31:1 (22)). In doing so, we sought to assess
621 whether the DFE estimates were sensitive to misspecification of this ratio, considering a
622 plausible value for mammals.

623 We focused on the deleterious DFE, with selection coefficients (*s*) ranging from $|s| = 10^{-8}$ to
624 0.5. In doing so, we considered any portion of the DFE smaller than 10^{-8} to be effectively
625 neutral and larger than 0.5 to be lethal and have a negligible probability of being polymorphic
626 in sample sizes considered in our study. Dominance coefficients are assumed to be $h = 0.5$,
627 thus implying additive fitness effects.

628 We investigated three distributions of selection coefficients: the standard gamma distribution
629 for DFEs (22, 49, 79); a mixture distribution where a proportion of variants are neutral, with

16

630 the remaining variants with selection coefficients following a gamma distribution
631 ("neugamma"); and the bivariate lognormal distribution, the latter exclusively for the joint
632 estimation of DFE for each two pairs of populations (namely AW-BC, AW-LB, and AW-PG;
633 see below). For the neugamma distribution, the neutral mass and the gamma distribution can
634 effectively be treated as a single integrable function. The reported s are scaled by the inferred
635 ancestral population size estimated according to the demographic inference using the SFS of
636 synonymous variants, unless otherwise noted (e.g., Fig. S13). To discretize the DFE using the
637 estimated parameters of the distributions, we computed the cumulative probability in a given
638 range of s using the *pgamma* function in R.

639 *varDFE* outputs the standard deviation of the maximum likelihood parameter estimates
640 (MLEs) based on the Fisher's Information Matrix method implemented in $\partial a \partial i$, which we then
641 used to calculate confidence intervals using R. To do so, we assumed the MLEs of the shape
642 and scale parameters of the gamma distribution were normally distributed with means equal to
643 the maximum likelihood values and standard deviation as computed by *varDFE*. We then drew
644 10,000 shape and scale parameters using the function *pnorm* in R and used *pgamma* to compute
645 the discretized DFE for each replicate. The 95% confidence interval for each bin was taken as
646 the middle 95% of the simulated values.

647 We note that the maximum likelihood estimates for the scale parameter of the gamma
648 distribution reached the upper boundary during the DFE inferences in some instances (see
649 Tables S2 and S3), with uncertain biological significance. We initially used a range for the
650 scale parameter based on previous works with different organisms and slowly increased the
651 upper bound of the scale parameter until we reached 1,000,000. Reaching this upper bound
652 may be due to an innately highly deleterious DFE in canids. Importantly, the fit of the model
653 SFS to the data is satisfactory using this upper bound (Fig. S8-S11). The same phenomenon
654 was observed by Lin et al. (56) in an independent analysis of the AW data used in this study,
655 as well as for a population of Russian Karelian gray wolf not analyzed here. In addition,
656 Gaughran (80) describes the same phenomenon for the DFE estimates of the northern elephant
657 seal and the Baltic ringed seal.

658 **2D Demographic and DFE Inferences.** We inferred the joint DFE of pairs of populations:
659 AW-BC, AW-LB, and AW-PG. We assume the wolf and the breed dog populations recently
660 split form one another, and that there is symmetric gene flow between them. We also assume
661 that the wolf population is more similar to the ancestral population and keeps the same selection
662 coefficients while the diverged dog population may have different selection coefficients.

663 We inferred the demographic history and joint DFE using the joint SFS, which is a matrix in
664 which each entry is the count of the number of variants observed at frequency i in population
665 1 and j in population 2. Similar to the 1D analysis, here we also used the folded allele frequency
666 spectrum that counts the minor allele frequency. Different demographic histories and different
667 combinations of selection coefficients of two populations lead to distinct patterns in the joint
668 SFS (23).

17

669   We infer the demographic model using the joint SFS from synonymous variants. We assume
670   the ancestral population split into a wolf (AW) and a breed dog (BC, LB, or PG) population.
671   The derived populations after the split may have different population sizes among themselves
672   and relative to the ancestral population. Gene flow is assumed to be symmetric.

673   Since the DFE for single populations were found to be similar, we fit the joint DFE with a
674   symmetric bivariate lognormal model that is a joint distribution of correlated lognormal
675   variables (mean μ and standard deviation σ) with identical marginal distributions. That is, the
676   marginal DFE for the wolf population and dog population are the same, while the parameter ρ
677   quantifies the correlation of fitness effects of mutations between populations.

678   We used $\partial a \partial i / fit \partial a \partial i$ and the command line tool dadi-cli to infer the 2D demographic
679   model and the joint DFE. The parameters and commands used for inference can be found at
680   https://github.com/chenludi/canids_2DDFE_2024/tree/main.

681   **Gene Set Data.** The AmiGO Gene Ontology (GO) database
682   (https://amigo.geneontology.org/amigo) was accessed on 09/12/2024 for the retrieval of
683   information regarding gene names included in GO terms putatively associated with
684   domestication. These include "nervous system development" (GO:0007399), "immune system
685   process" (GO:0002376), "carbohydrate metabolic process" (GO:0005975), "pigmentation"
686   (GO:0043473), and "skeletal system development" (GO:0001501). The choice for those
687   specific five GO terms sought to balance the specificity of the term with the number of genes
688   included in each. The data was filtered considering *"Canis lupus familiaris"* as "Organism."
689   From these, we obtained the relevant gene IDs based on the "gene/product (bioentity label)"
690   column. The coordinates for the selected genes were obtained from the UCSC Genome
691   Browser
692   (https://hgdownload.soe.ucsc.edu/goldenPath/canFam3/bigZips/genes/canFam3.ncbiRefSeq.g
693   tf.gz), accessed on 09/05/2024. Exon length for each gene set was 5,761,394 bp, 3,703,799 bp,
694   1,060,844 bp, 239,818 bp, and 1,254,685 bp respectively. We considered "nervous system
695   development" and "immune system process" separately, and also merged all five gene sets into
696   a "domestication-associated genes" set for a total of 10,483,822 bp. Data processing and
697   subsetting were performed with in-house scripts, as well as *BCFtools* (81) and *BEDtools* (82).

698   **A Recombination Map for the Arctic Wolf.**

699   To infer a fine-scale recombination map for the AW, we used the unphased high coverage
700   polymorphism data used for the DFE inference as described above. The map was built based
701   on linkage disequilibrium (LD) patterns across the genome. To do so, we first inferred AW
702   demographic history (i.e., changes in N_e through time) with SMC++ (83), considering all 38
703   autosomal chromosomes. We considered a mutation rate of 4.5e-9 per base pair per generation,
704   based on a wolf pedigree study (84). Then, we estimated the recombination rate per-
705   chromosome using *pyrho* (85). When computing a lookup table in *pyrho*, we used the manual
706   recommendation of calculating statistics of LD and *rho* (population recombination rate) based
707   on a population size that was 50% larger than our sample size. For the final step of inferring
708   recombination rates (*r*) in *pyrho*, we used a window size and block penalty of 50.

18

Assessing DFE Variation as a Function of Recombination Rate. We used the LD-based recombination map that we inferred for the AW to split its genome into three different bins based on r in units of per bp per generation and considering non-overlapping 1 MB windows: Low ($0 \leq r < 1.9e\text{-}9$), Moderate ($1.9e\text{-}9 \leq r < 4.3e\text{-}9$), and High ($r \geq 4.3e\text{-}9$) recombination rate. We excluded regions with recombination rates above 2e-8 per bp per generation. In doing so, we sought to have approximately equal amounts of data (in base pairs) across the three bins. As a result, each bin contained roughly ⅓ the number of synonymous and nonsynonymous SNPs found across all exons. Considering each of the three recombination bins separately, we inferred demographic history and the gamma DFE using the same approach implemented for the whole exome data.

Acknowledgments

References

1. L. A. F. Frantz, D. G. Bradley, G. Larson, L. Orlando, Animal domestication in the era of ancient genomics. *Nat. Rev. Genet.* **21**, 449–460 (2020).

2. J. Lu, *et al.*, The accumulation of deleterious mutations in rice genomes: a hypothesis on the cost of domestication. *Trends Genet.* **22**, 126–131 (2006).

3. J. F. Doebley, B. S. Gaut, B. D. Smith, The molecular genetics of crop domestication. *Cell* **127**, 1309–1321 (2006).

4. B. T. Moyers, P. L. Morrell, J. K. McKay, Genetic costs of domestication and improvement. *J. Hered.* **109**, 103–116 (2018).

5. C. D. Marsden, *et al.*, Bottlenecks and selective sweeps during domestication have increased deleterious genetic variation in dogs. *Proc. Natl. Acad. Sci. U. S. A.* **113**, 152–157 (2016).

6. T. Makino, *et al.*, elevated proportions of deleterious genetic variation in domestic animals and plants. *Genome Biol. Evol.* **10**, 276–290 (2018).

7. M. Schubert, *et al.*, Prehistoric genomes reveal the genetic foundation and cost of horse domestication. *Proc. Natl. Acad. Sci. U. S. A.* **111**, E5661–E5669 (2014).

8. J. A. Mooney, A. Yohannes, K. E. Lohmueller, The impact of identity by descent on fitness and disease in dogs. *Proc. Natl. Acad. Sci. U. S. A.* **118** (2021).

9.   A. R. Boyko, *et al.*, A simple genetic architecture underlies morphological variation in dogs. *PLoS Biol.* **8**, e1000451 (2010).

10. J. Ross-Ibarra, The evolution of recombination under domestication: a test of two hypotheses. *Am. Nat.* **163**, 105–112 (2004).

11. R. R. Fuentes, D. de Ridder, A. D. J. van Dijk, S. A. Peters, Domestication shapes recombination patterns in tomato. *Mol. Biol. Evol.* **39** (2022).

12. F. J. Alberto, *et al.*, Convergent genomic signatures of domestication in sheep and goats. *Nat. Commun.* **9**, 813 (2018).

13. A. Vaysse, *et al.*, Identification of genomic regions associated with phenotypic variation between dog breeds using selection mapping. *PLoS Genet.* **7**, e1002316 (2011).

14. A. Eyre-Walker, P. D. Keightley, The distribution of fitness effects of new mutations. *Nat. Rev. Genet.* **8**, 610–618 (2007).

15. A. Eyre-Walker, Genetic architecture of a complex trait and its implications for fitness and genome-wide association studies. *Proc. Natl. Acad. Sci. U. S. A.* **107**, 1752–1756 (2010).

16. C. C. Kyriazis, J. A. Robinson, K. E. Lohmueller, Using computational simulations to model deleterious variation and genetic load in natural populations. *Am. Nat.* (2023). https://doi.org/10.1086/726736.

17. N. H. Barton, A general model for the evolution of recombination. *Genet. Res.* **65**, 123–145 (1995).

18. D. Castellano, M. Coronado-Zamora, J. L. Campos, A. Barbadilla, A. Eyre-Walker, Adaptive evolution is substantially impeded by Hill-Robertson interference in Drosophila. *Mol. Biol. Evol.* **33**, 442–455 (2016).

19. T. I. Gossmann, P. D. Keightley, A. Eyre-Walker, The effect of variation in the effective population size on the rate of adaptive molecular evolution in eukaryotes. *Genome Biol. Evol.* **4**, 658–667 (2012).

20. D. Charlesworth, B. Charlesworth, M. T. Morgan, The pattern of neutral molecular variation under the background selection model. *Genetics* **141**, 1619–1632 (1995).

21. J. Chen, T. Bataillon, S. Glémin, M. Lascoux, What does the distribution of fitness effects of new mutations reflect? Insights from plants. *New Phytol.* **233**, 1613–1619 (2022).

22. C. D. Huber, B. Kim, C. D. Marsden, K. E. Lohmueller, Determining the factors driving selective effects of new nonsynonymous mutations. *Proc. Natl. Acad. Sci. U. S. A.* **114**, 4465–4470 (2017).

23. X. Huang, *et al.*, Inferring genome-wide correlations of mutation fitness effects between populations. *Mol. Biol. Evol.* **38**, 4588–4602 (2021).

24. D. Castellano, M. C. Macià, P. Tataru, T. Bataillon, K. Munch, Comparison of the full distribution of fitness effects of new amino acid mutations across great apes. *Genetics* **213**, 953–966 (2019).

25. J. Lourenço, N. Galtier, S. Glémin, Complexity, pleiotropy, and the fitness effect of mutations. *Evolution* **65**, 1559–1571 (2011).

26. R. A. Goldstein, Population size dependence of fitness effect distribution and substitution rate

probed by biophysical model of protein thermostability. *Genome Biol. Evol.* **5**, 1584–1593 (2013).

27. J. A. Mooney, C. D. Marsden, A. Yohannes, R. K. Wayne, K. E. Lohmueller, Long-term small population size, deleterious variation, and altitude adaptation in the Ethiopian wolf, a severely endangered canid. *Mol. Biol. Evol.* **40** (2023).

28. J. Chen, S. Glémin, M. Lascoux, Genetic diversity and the efficacy of purifying selection across plant and animal species. *Mol Biol Evol* **34**, 1417–1428 (2017).

29. A. H. Freedman, *et al.*, Genome sequencing highlights the dynamic early history of dogs. *PLoS Genet.* **10**, e1004016 (2014).

30. M. M. Gray, *et al.*, Linkage disequilibrium and demographic history of wild and domestic canids. *Genetics* **181**, 1493–1505 (2009).

31. G. Larson, D. Q. Fuller, The evolution of animal domestication. *Annu. Rev. Ecol. Evol. Syst.* **45**, 115–136 (2014).

32. A. V. Kukekova, *et al.*, Red fox genome assembly identifies genomic regions associated with tame and aggressive behaviours. *Nat Ecol Evol* **2**, 1479–1491 (2018).

33. M. Lahtinen, D. Clinnick, K. Mannermaa, J. S. Salonen, S. Viranta, Excess protein enabled dog domestication during severe Ice Age winters. *Sci. Rep.* **11**, 7 (2021).

34. P. Skoglund, E. Ersmark, E. Palkopoulou, L. Dalén, Ancient wolf genome reveals an early divergence of domestic dog ancestors and admixture into high-latitude breeds. *Curr. Biol.* **25**, 1515–1519 (2015).

35. L. A. F. Frantz, *et al.*, Genomic and archaeological evidence suggest a dual origin of domestic dogs. *Science* **352**, 1228–1231 (2016).

36. H. G. Parker, *et al.*, Genomic analyses reveal the influence of geographic origin, migration, and hybridization on modern dog breed development. *Cell Rep.* **19**, 697–708 (2017).

37. K. Lindblad-Toh, *et al.*, Genome sequence, comparative analysis and haplotype structure of the domestic dog. *Nature* **438**, 803–819 (2005).

38. J. A. Robinson, *et al.*, Genomic signatures of extensive inbreeding in Isle Royale wolves, a population on the threshold of extinction. *Sci Adv* **5**, eaau0757 (2019).

39. T. N. Phung, R. K. Wayne, M. A. Wilson, K. E. Lohmueller, Complex patterns of sex-biased demography in canines. *Proc. Biol. Sci.* **286**, 20181976 (2019).

40. J. Plassais, *et al.*, Whole genome sequencing of canids reveals genomic regions under selection and variants influencing morphology. *Nature Communications* **10**, 1489 (2019).

41. T. W. Marchant, *et al.*, Canine brachycephaly is associated with a retrotransposon-mediated missplicing of smoc2. *Current Biology* **27**,1573-1584.e6 (2017).

42. B. Y. Kim, C. D. Huber, K. E. Lohmueller, Inference of the distribution of selection coefficients for new nonsynonymous mutations using large samples. *Genetics* **206**, 345–361 (2017).

43. R. N. Gutenkunst, R. D. Hernandez, S. H. Williamson, C. D. Bustamante, Inferring the joint demographic history of multiple populations from multidimensional SNP frequency data. *PLoS Genetics* **5**, e1000695 (2009).

825   44. K. A. Lord, G. Larson, R. P. Coppinger, E. K. Karlsson, The history of Farm Foxes undermines
826   the animal domestication syndrome. *Trends Ecol. Evol.* **35**, 125–136 (2020).

827   45. H. Ai, *et al.*, Human-mediated admixture and selection shape the diversity on the modern swine
828   (*Sus scrofa*) Y chromosomes. *Mol. Biol. Evol.* **38**, 5051–5065 (2021).

829   46. M. J. Montague, *et al.*, Comparative analysis of the domestic cat genome reveals genetic
830   signatures underlying feline biology and domestication. *Proc. Natl. Acad. Sci. U. S. A.* **111**,
831   17230–17235 (2014).

832   47. Y. Zhen, C. D. Huber, R. W. Davies, K. E. Lohmueller, Greater strength of selection and higher
833   proportion of beneficial amino acid changing mutations in humans compared with mice and.
834   *Genome Res* **31**, 110–120 (2021).

835   48. X. Ma, *et al.*, Population genomic analysis reveals a rich speciation and demographic history of
836   orang-utans (*Pongo pygmaeus* and *Pongo abelii*). *PLoS ONE* **8**, e77175 (2013).

837   49. A. R. Boyko, *et al.*, Assessing the evolutionary impact of amino acid mutations in the human
838   genome. *PLoS Genet.* **4**, e1000083 (2008).

839   50. A. D. Wang, N. P. Sharp, A. F. Agrawal, Sensitivity of the distribution of mutational fitness
840   effects to environment, genetic background, and adaptedness: a case study with Drosophila.
841   *Evolution* **68**, 840–853 (2014).

842   51. R. Kishony, S. Leibler, Environmental stresses can alleviate the average deleterious effect of
843   mutations. *J Biol* **2**, 14 (2003).

844   52. X. Huang, S. Wang, L. Jin, Y. He, Dissecting dynamics and differences of selective pressures in
845   the evolution of human pigmentation. *Biol Open* **10** (2021).

846   53. D. Castellano, I.-T. Vourlaki, R. N. Gutenkunst, S. E. Ramos-Onsins, Detection of domestication
847   signals through the analysis of the full distribution of fitness effects using simulations. *bioRxiv*
848   2022.08.24.505198 (2024).

849   54. P. Sahlén, *et al.*, Variants that differentiate wolf and dog populations are enriched in regulatory
850   elements. *Genome Biol Evol* **13** (2021).

851   55. A. Couce, *et al.*, Changing fitness effects of mutations through long-term bacterial evolution.
852   *Science* **383**, eadd1417 (2024).

853   56. M. Lin *et al.,* The distribution of fitness effects varies phylogenetically across animals. *bioRxiv*

854   57. O. Tenaillon, The utility of Fisher's geometric model in evolutionary genetics. *Annu Rev Ecol*
855   *Evol Syst* **45**, 179–201 (2014).

856   58. A. Auton, *et al.*, Genetic recombination is targeted towards gene promoter regions in dogs. *PLoS*
857   *Genet* **9**, e1003984 (2013).

858   59. F. Baudat, *et al.*, PRDM9 is a major determinant of meiotic recombination hotspots in humans
859   and mice. *Science* **327**, 836–840 (2010).

860   60. B. de Massy, Initiation of meiotic recombination: how and where? Conservation and specificities
861   among eukaryotes. *Annu Rev Genet* **47**, 563–599 (2013).

862   61. J. Felsenstein, The evolutionary advantage of recombination. *Genetics* **78**, 737–756 (1974).

863   62. H. J. Muller, The relation of recombination to mutational advance. *Mutat Res* **106**, 2–9 (1964).

864   63. H. Li, R. Durbin, Fast and accurate short read alignment with Burrows-Wheeler transform.
865   *Bioinformatics* **25**, 1754–1760 (2009).

866   64. P. Danecek, *et al.*, Twelve years of SAMtools and BCFtools. *GigaScience* **10**, giab008 (2021).

867   65. G. A. V. der Auwera, *et al.*, From FastQ data to high-confidence variant calls: The Genome
868   Analysis Toolkit best practices pipeline. *Current Protocols in Bioinformatics* **43**, 11.10.1-
869   11.10.33 (2013).

870   66. G. A. Van der Auwera, B. D. O'Connor, *Genomics in the Cloud: Using Docker, GATK, and*
871   *WDL in Terra* (O'Reilly Media, 2020).

872   67. P. Danecek, *et al.*, The variant call format and VCFtools. *Bioinformatics* **27**, 2156–2158 (2011).

873   68. P. Cingolani, Variant annotation and functional prediction: SnpEff. *Methods Mol. Biol.* **2493**,
874   289–314 (2022).

875   69. P. Cingolani, *et al.*, A program for annotating and predicting the effects of single nucleotide
876   polymorphisms, SnpEff. *Fly* **6**, 80-92 (2012).

877   70. A. Manichaikul, *et al.*, Robust relationship inference in genome-wide association studies.
878   *Bioinformatics* **26**, 2867–2873 (2010).

879   71. S. Purcell, *et al.*, PLINK: A tool set for whole-genome association and population-based linkage
880   analyses. *The American Journal of Human Genetics* **81**, 559–575 (2007).

881   72. R. D. Hernandez, S. H. Williamson, C. D. Bustamante, Context dependence, ancestral
882   misidentification, and spurious signatures of natural selection. *Mol. Biol. Evol.* **24**, 1792–1800
883   (2007).

884   73. A. Kong, *et al.*, Rate of de novo mutations and the importance of father's age to disease risk.
885   *Nature* **488**, 471–475 (2012).

886   74. A. P. Bird, DNA methylation and the frequency of CpG in animal DNA. *Nucleic Acids Research*
887   **8**, 1499–1504 (1980).

888   75. B. M. Neale, *et al.*, Patterns and rates of exonic de novo mutations in autism spectrum disorders.
889   *Nature* **485**, 242–245 (2012).

890   76. P. Moorjani, C. E. G. Amorim, P. F. Arndt, M. Przeworski, Variation in the molecular clock of
891   primates. *Proc. Natl. Acad. Sci. U. S. A* **113**, 10607-10612 (2016).

892   77. L. Han, Z. Zhao, Contrast features of CpG islands in the promoter and other regions in the dog
893   genome. *Genomics* **94**, 117–124 (2009).

894   78. P. W. Messer, D. A. Petrov, Frequent adaptation and the McDonald-Kreitman test. *Proc. Natl.*
895   *Acad. Sci. U. S. A.* **110**, 8615–8620 (2013).

896   79. A. Kousathanas, P. D. Keightley, A comparison of models to infer the distribution of fitness
897   effects of new mutations. *Genetics* **193**, 1197-1208 (2013).

898   80. S. J. Gaughran. *Patterns of Adaptive and Purifying Selection in the Genomes of Phocid Seals*.
899   PhD thesis. United States – Connecticut: Yale University, 2021. 197 pp. isbn: 9798534651188.

900   81. H. Li, A statistical framework for SNP calling, mutation discovery, association mapping and
901   population genetical parameter estimation from sequencing data. *Bioinformatics* **27**, 2987–2993
902   (2011).

23

903   82. A. R. Quinlan, I. M. Hall, BEDTools: a flexible suite of utilities for comparing genomic features.
904   *Bioinformatics* **26**, 841–842 (2010).

905   83. J. Terhorst, J. A. Kamm, Y. S. Song, Robust and scalable inference of population history from
906   hundreds of unphased whole genomes. *Nat Genet* **49**, 303–309 (2017).

907   84. E. M. Koch, *et al.*, De novo mutation rate estimation in wolves of known pedigree. *Mol Biol Evol*
908   **36**, 2536–2547 (2019).

909   85. J. P. Spence, Y. S. Song, Inference and analysis of population-specific fine-scale recombination
910   maps across 26 diverse human populations. *Sci Adv* **5**, eaaw9206 (2019).

911

912 **Figures**
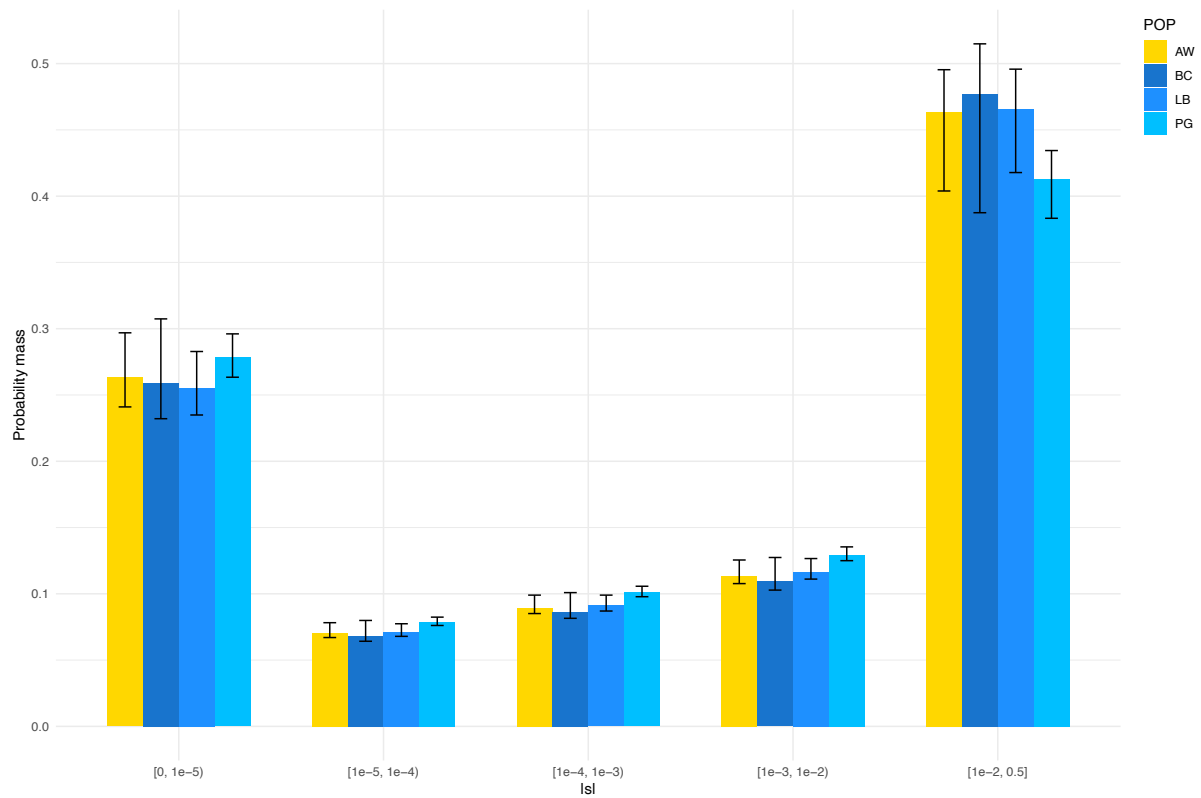
913

914 Fig. 1. Discretized distribution of fitness effects (DFE) showing the proportions of
915 nonsynonymous mutations in various categories of $|s|$. From left to right, mutations range from
916 neutral/nearly neutral ($0 < |s| \leq$ 1e-5) to strongly deleterious/lethal ($|s| \geq$ 1e-2). The DFE is
917 assumed to follow a gamma distribution. The arctic wolf population (AW) is depicted in
918 yellow, and three domestic dog breeds in different shades of blue (BC = border collie; LB =
919 labrador retriever; PG = pug). Error bars represent the 95% confidence intervals for the
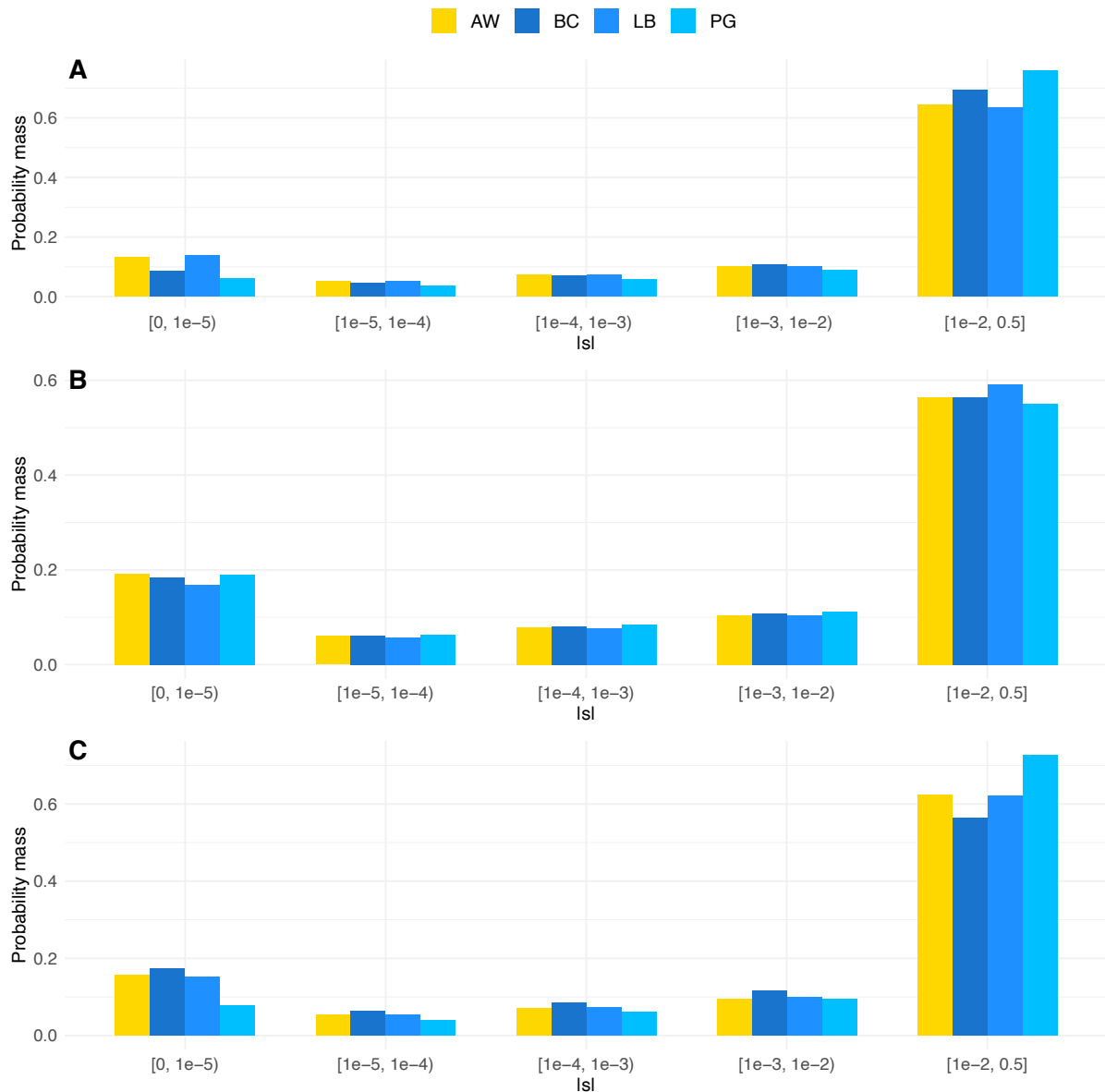920 proportion of mutations in each category of $|s|$.

Fig. 2. Discretized distribution of fitness effects (DFE) showing the proportions of nonsynonymous mutations in various categories of |s| for different gene sets: (A) Nervous System Development, (B) Immune System Processes, and (C) a combination of Immune System Processes, Nervous System Development, Carbohydrate Metabolic Processes, Pigmentation, and Skeletal System Development ("Domestication Genes" subset). In all panels, mutations range from neutral/nearly neutral ($1e{-}5 < |s| \leq 0$) to strongly deleterious/lethal ($|s| \geq 1e{-}2$). The DFE is assumed to follow a gamma distribution. The arctic wolf population (AW) is depicted in yellow, and three different domestic dog breeds in different shades of blue (BC = border collie; LB = labrador retriever; PG = pug). Confidence intervals for these estimates can be found in Table S6.

934 **Table**

Population comparison	Proportions of nonsynonymous mutations in various categories of $|s|$					ρ^{a}	F_{ST}^{b}
	[0, 1e-5)	[1e-5, 1e-4)	[1e-4, 1e-3)	[1e-3, 1e-2)	[1e-2, 0.5)		
AW	26%	7%	9%	11%	46%	n/a	n/a
BC	26%	7%	9%	11%	48%	n/a	n/a
LB	26%	7%	9%	12%	47%	n/a	n/a
PG	28%	8%	10%	13%	41%	n/a	n/a
AW-BC	20%	8%	9%	10%	53%	0.999	0.166
AW-LB	21%	7%	8%	8%	56%	0.999	0.175
AW-PG	21%	8%	9%	9%	54%	0.999	0.234

935 Table 1. Comparison of the proportions of nonsynonymous mutations in various categories of
936 $|s|$. Shown are the estimates for the Arctic wolf (AW), border collie (BC), labrador retriever
937 (LB), and pug (PG) considering the 1D site frequency spectrum (SFS) and for each pair of
938 populations including AW and each of the three dog breeds based on the 2D SFS. The AW's
939 DFE is assumed to be gamma-distributed, while the joint DFEs are assumed to be lognormal
940 distributed. [a]ρ represents the correlation coefficient of the DFE between pairs of populations.
941 [b]F_{ST} from ref. (27).